

# Semisynthesis and Screening of a Small Library of Pro-Apoptotic Squamocin Analogues: Selection and Study of a Benzoquinone Hybrid with an Improved Biological Profile.

S  verine Derbr  ,<sup>[a]</sup> Romain Duval,<sup>[a]</sup> Ga  l Rou  ,<sup>[b]</sup> Aurelio Garofano,<sup>[c]</sup> Erwan Poupon,<sup>\*,[a]</sup> Ulrich Brandt,<sup>[c]</sup> Santos A. Susin,<sup>\*,[b]</sup> and Reynald Hocquemiller<sup>[a]</sup>

Acetogenins of Annonaceae, including squamocin (**1**), exert spectacular cytotoxicity and the most potent inhibition of NADH:ubiquinone oxidoreductase known so far. Cell death induced by these natural products was identified as apoptosis and was thought to be linked to alterations in mitochondrial function. Quinone–squamocin hybrid compounds were semisynthesized and evaluated for their pro-apoptotic properties with a screening method based on dissipation of the mitochondrial transmem-

brane potential ( $\Delta\Psi_m$ ). Herein, we report a short one-step synthesis of a squamocin carboxylic acid analogue. For the first time on a natural product, the radical decarboxylation and quinone addition reaction has enabled preparation of a library of squamocin–quinone hybrids and four other analogues. Squamoquinone, tenfold more potent than squamocin as an inducer of apoptosis, emerged as a promising compound, as it induces apoptosis through a mitochondrial caspase-dependent pathway.

## Introduction

The acetogenins are a class of natural products of the *Annonaceae* plant family. They exert a wide variety of biological activities, including an impressive cytotoxicity ( $IC_{50}$  between  $10^{-6}$  and  $10^{-14}$  M), which has been reported on various tumor cell lines, and a very powerful inhibition of complex I (NADH:ubiquinone oxidoreductase) in mitochondrial transport systems.<sup>[1]</sup> In addition, cell death induced by some mono- and bis-tetrahydrofuran acetogenins has been described over the past few years as an apoptotic process.<sup>[2–4]</sup> Some mitochondrial respiratory-chain inhibitors such as rotenone, antimycin A, and oligomycin have already been implicated in programmed cell death independently of the expression of the anti-apoptotic protein Bcl-2, suggesting a direct link between the inhibition of mitochondrial respiration and apoptosis.<sup>[5]</sup> The development of acetogenin derivatives as anti-neoplastic agents, for example, also relies on the elucidation of their modes of action and their selectivity on the cell cycle. This latter point is important, as the natural acetogenins exhibit their promising cytotoxicity despite a complete absence of selectivity toward the cell cycle.<sup>[6]</sup>

The  $\alpha,\beta$ -unsaturated  $\gamma$ -methylbutyrolactone ring, which is common to a large number of natural acetogenins, is not essential for complex I inhibition,<sup>[7,8]</sup> as it can be suppressed<sup>[9]</sup> or substituted with a ubiquinone ring.<sup>[10,11]</sup> By synthesizing fluorescent acetogenin derivatives, we recently demonstrated the role of the terminal part of acetogenins in the pro-apoptotic activity as well. The bis-tetrahydrofuran motif flanked with hydroxy groups and lipophilic chains was confirmed to be involved in the recruitment of the molecule almost exclusively to mitochondrial membranes.<sup>[12]</sup>

To improve the acetogenin profile as a therapeutic agent and to elucidate the acetogenin mechanisms of action, squamocin (**1**, a powerful cytotoxic bis-tetrahydrofuran acetogenin and an inhibitor of complex I, Figure 1) was selected for the semisynthesis of quinone–squamocin hybrid compounds.

It has been shown that exchange of the terminal butenolide unit with 2,3-dimethoxy-5-methylbenzoquinone in different acetogenins makes it possible to either maintain<sup>[11]</sup> or increase<sup>[10]</sup> the potency of complex I inhibition, as the  $\gamma$ -lactone group is completely substitutable with the ubiquinone ring.

[a] S. Derbr  , Dr. R. Duval, Dr. E. Poupon, Prof. R. Hocquemiller  
Laboratoire de Pharmacognosie associ   au CNRS  
(BioCIS, UMR 8076)  
Universit   Paris-Sud 11  
Centre d'  tudes Pharmaceutiques  
5 rue Jean-Baptiste Cl  ment  
92296 Ch  tenay-Malabry CEDEX (France)  
Fax: (+ 33) 1-46-83-53-99  
E-mail: erwan.poupon@cep.u-psud.fr

[b] Dr. G. Rou  , Dr. S. A. Susin  
Groupe Apoptose et Syst  me Immunitaire  
CNRS-URA 1961, Institut Pasteur  
25 rue du Dr. Roux, 75015 Paris (France)  
Fax: (+ 33) 1-40-61-31-86  
E-mail: susin@pasteur.fr

[c] Dr. A. Garofano, Prof. U. Brandt  
Institut f  r Biochemie I, Fachbereich Medizin  
Universit  t Frankfurt  
60590 Frankfurt am Main (Germany)

Supporting information for this article is available on the WWW under <http://www.chemmedchem.org> or from the author.

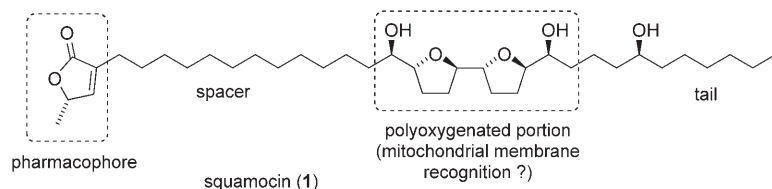


**Figure 1.** Structure of squamocin (**1**, isolated from the seeds of *Annona reticulata*). Simplified structure–activity relationship elements are indicated.<sup>[49, 54]</sup>

Furthermore, several quinones with antitumor activity have been implicated in the induction of apoptosis,<sup>[13]</sup> as have been acetogenins. Any study of cytotoxicity or apoptotic potential of semisynthetic acetogenin–quinone compounds has yet to be reported or envisaged in published work to date. Consequently, we decided to embark upon the design of new squamocin analogues with a focus on the replacement of the unsaturated lactone with diverse quinone rings. Starting from natural squamocin, selective and reliable synthetic methods had to be chosen carefully to enable the transformation of small amounts of substrate.

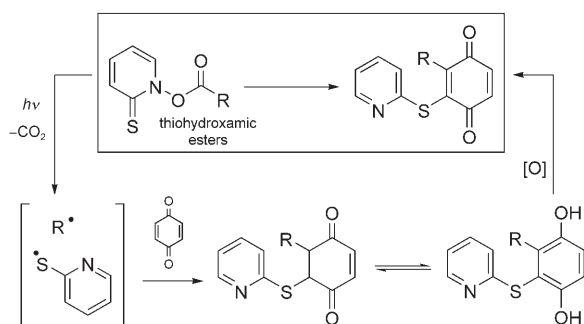
The pro-apoptotic potential of squamocin and quinone derivatives was evaluated on Jurkat lymphoid T cells by screening the induction of the disruption of mitochondrial transmembrane potential ( $\Delta\Psi_m$ ), one of the first biochemical hallmarks of the apoptotic process.<sup>[14–16]</sup> Squamoquinone **14**, tenfold more efficient than natural squamocin, emerged as a promising compound. The molecule has been selected for further studies of its pro-apoptotic properties relative to those of squamocin (**1**).

## Results and Discussion

### Semisynthesis and retrosynthetic analysis

In 1987, Barton and co-workers expanded the practicality of radical decarboxylation to the synthesis of sterically hindered quinones. This involves the effective “substitution” of one carboxylic acid function by a quinone. The concept of the reaction is based on the generation of a radical from a photosensitive thiohydroxamic ester and the subsequent trapping by a quinone in a disciplined radical chain reaction (Scheme 1).<sup>[17,18]</sup>

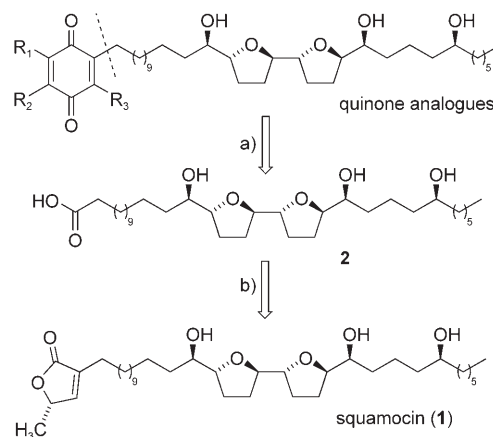
Herein, we broaden the scope of this reaction to the modification of natural compounds. To our knowledge, this is the



**Scheme 1.** Radical decarboxylation and quinone addition reaction.

first time the reaction has been applied in a semisynthesis context, and on high molecular weight scaffolds as well. As stated above, our synthetic plan relies on the availability of a carboxylic acid function such as that in **2**, derived from squamocin. Therefore, this required a convenient oxidative degradation of the terminal lactone ring in **1** (Scheme 2).

**Squamocin carboxylic acid synthesis.** Recently,  $\alpha$ -ketoester and  $\alpha$ -ketoacid derivatives of squamocin

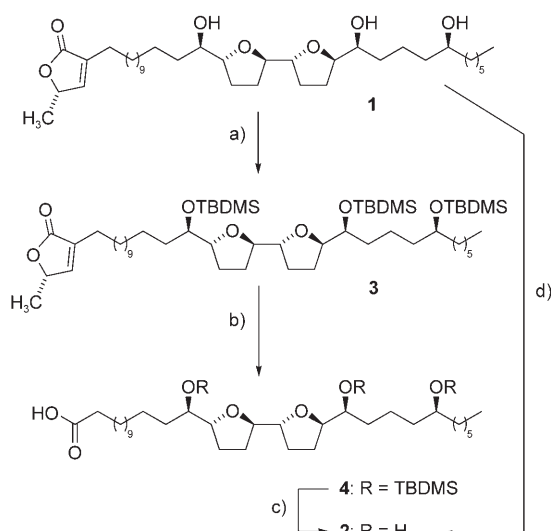


**Scheme 2.** Retrosynthetic analysis: a) radical decarboxylation and quinone addition (----); b) new oxidative degradation.

were obtained from the *tert*-butyldimethylsilyl (TBDMS) ether of squamocin **3** after oxidative treatment with sodium periodate and catalytic ruthenium chloride.<sup>[19]</sup>

Inexpensive and less toxic potassium permanganate appeared to be a suitable alternative for obtaining the  $\alpha$ -ketoester from terminal butenolide by olefin oxidation. Squamocin (**1**) was first protected as its tri-OTBDMS silylether derivative **3**. Surprisingly, treatment of protected squamocin **3** with  $\text{KMnO}_4$  (4 equiv) in acetone/water (5:1) at room temperature overnight led to the squamocin–acid derivative **4** directly and cleanly with a good yield of 70% (Scheme 3). More gratifyingly, the same oxidation reaction could be applied directly to the natural squamocin (**1**) without hydroxy group protection to effect the same three-carbon loss in just one step. This afforded acid **2** in a lower but acceptable 60% yield.

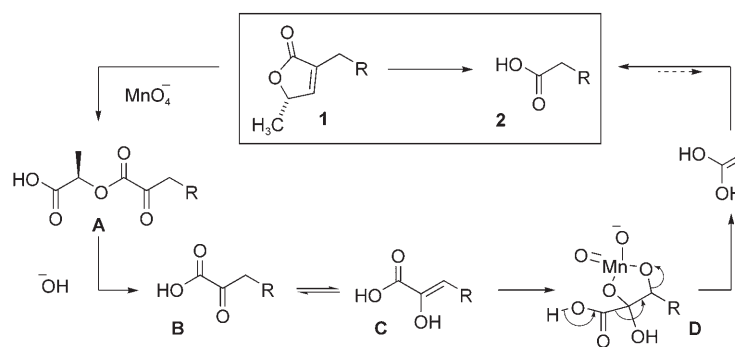
Even if  $\alpha$ -ketoester of type **A** (Scheme 4) was not isolated, the following mechanism can be proposed. First, as was described with the ruthenium-catalyzed periodic oxidation of acetogenin butyrolactone, permanganate anions could provoke the oxidation of the  $\alpha,\beta$ -unsaturated  $\gamma$ -methylbutyrolactone olefin to afford lactic  $\alpha$ -ketoester **A** in the method commonly used to obtain the corresponding lactate and to determine the absolute configuration of C36.<sup>[20,21]</sup> Hydrolysis of **A** furnishes  $\alpha$ -ketoacid **B** (two carbon atoms are lost in this step). As was previously described with calcium hypochlorite<sup>[22]</sup> and sodium perborate,<sup>[23]</sup> such  $\alpha$ -ketoacids can be decarboxylated under oxidative conditions. In fact, the resulting keto tautomer **B** is in equilibrium with the corresponding enol form **C**. This allows reaction with a second molecule of permanganate and



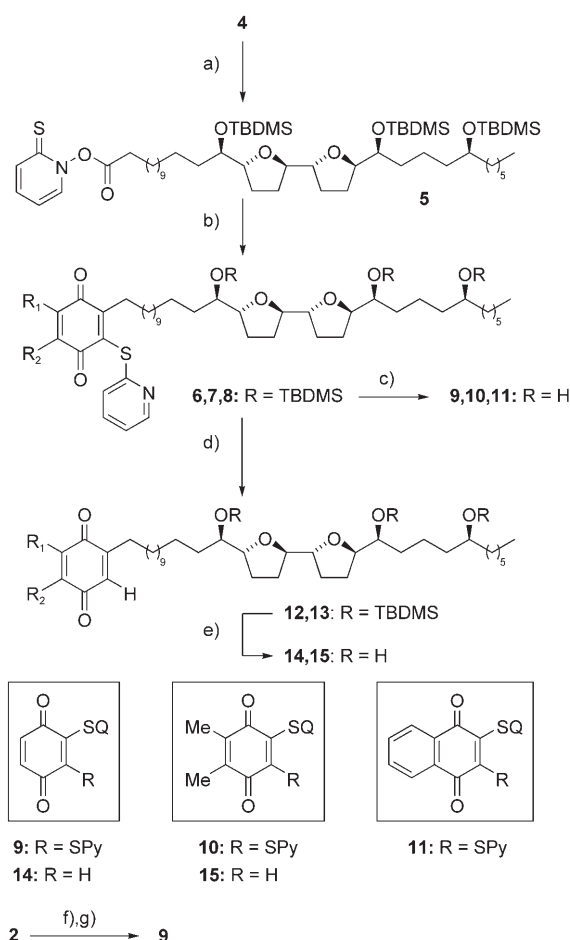
**Scheme 3.** Degradation of the lactone into a carboxylic acid group: a) TBDMSOTf (4.0 equiv), DMAP (cat.), pyridine, RT, 2 h (80%); b)  $\text{KMnO}_4$  (4 equiv),  $\text{H}_2\text{O}/\text{acetone}$  (1:5), RT, 24 h (70%); c) TBAF (1 M in THF, 100 equiv),  $50^\circ\text{C}$ , 6 h (90%); d)  $\text{KMnO}_4$  (4 equiv),  $\text{H}_2\text{O}/\text{acetone}$  (1:5), RT, 24 h (60%). DMAP = 4-(dimethylamino)pyridine; TBAF = tetra-*n*-butylammonium fluoride; TBDMSOTf = *tert*-butyldimethylsilyl trifluoromethanesulfonate.

the formation of an unstable intermediate **D**, which is further decarboxylated to afford squamocin-acid derivative **E/2**.<sup>[23]</sup>

*Chimeric squamocin-quinone compounds through radical decarboxylation and quinone addition.* For reasons of polarity, we first decided to target the quinone analogues by starting with the less polar squamocin-acid **4**. Thus, thiopyridine-*N*-oxide (1.2 equiv) was condensed with **4** under classical coupling conditions (DCC, 4-DMAP (cat.)) to furnish thioxydroxamic ester **5** in 80% yield (Scheme 5). Exposure of **5** to light in  $\text{CH}_2\text{Cl}_2$  in the presence of the desired quinones (3 equiv) made the anticipated synthesis of protected squamocin-thiopyridylquinones **6–8** possible. This crucial photochemical step proceeded in acceptable to good and reproducible yields with the three selected quinones. The simple *p*-benzoquinone was selected first to test the feasibility of the reaction. This was followed by the use of 2,3-dimethylbenzoquinone and naphthoquinone. The use of symmetric quinones was found to be effective in avoiding problems in regioselectivity and in subsequent purification steps.



**Scheme 4.** Plausible mechanism of permanganate-mediated degradation of the  $\alpha,\beta$ -unsaturated  $\gamma$ -methylbutyrolactone olefin group to a carboxylic acid, as discussed in text.



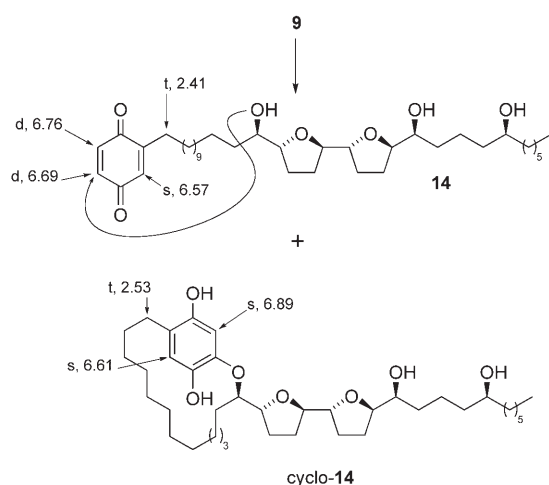
**Scheme 5.** Synthesis of quinones: a) thiopyridine-*N*-oxide (1.2 equiv), DCC (2 equiv), DMAP (cat.),  $\text{CH}_2\text{Cl}_2$ , RT, 24 h (80%); b)  $h\nu$ , quinone (3 equiv),  $\text{CH}_2\text{Cl}_2$ ,  $0-10^\circ\text{C}$ , 1–2 h (**6**: 51%, **7**: 54%, **8**: 39%); c) HF (75 equiv),  $\text{CH}_3\text{CN}/\text{CH}_2\text{Cl}_2$  (1:5), RT, 45 min (**9**: 86%, **10**: 43%, **11**: 97%); d) Raney nickel (10 equiv *m/m*), THF, reflux, 45 min (**12**: 69%, **13**: 80%); e) HF (75 equiv),  $\text{CH}_3\text{CN}/\text{CH}_2\text{Cl}_2$  (1:5), RT, 45 min (**14**: 70%, **15**: 77%); f) thiopyridine-*N*-oxide (20 equiv), DCC (2 equiv), DMAP (cat.),  $\text{CH}_2\text{Cl}_2$ , RT, 24 h (75%); g)  $h\nu$ , benzoquinone (3 equiv),  $\text{CH}_2\text{Cl}_2$ ,  $0-10^\circ\text{C}$ , 1 h (20%). DCC = 1,3-dicyclohexylcarbodiimide.

To evaluate the influence of the thiopyridyl moiety on biological activity, TBDMS-protected quinones **6–8** were subjected to either direct desilylation (Scheme 5, route c) or reductive desulfurization (route d)). In the former case, treatment with HF in  $\text{CH}_3\text{CN}/\text{CH}_2\text{Cl}_2$  (1:5) led to our first set of chimeric squamocin-thiopyridylbenzoquinones **9–11**. For the latter route, the thiopyridyl group attached to the quinone ring was removed under reductive conditions with an excess of Raney nickel in THF. The hydroquinone intermediates (not isolated) were immediately reoxidized to the corresponding quinones with  $\text{MnO}_2$  to obtain the second set of analogues after deprotection: squamocin-quinones **14–15** (70–80% yield).

Despite repeated efforts, the desulfurization of naphthoquinone adduct **11** was unsuccessful under the conditions used. Ultimately, we attempted to apply the radical decarboxylation directly to unpro-

tected squamocin–acid derivative **2**. To avoid the intramolecular lactonization with the reactive hydroxy group at C15, **2** was esterified with thiopyridine-*N*-oxide (20 equivalents) in the above-described coupling conditions to afford a 75% yield of the corresponding photosensitive thiohydroxamic ester. This ester was then decarboxylated upon exposure to light in  $\text{CH}_2\text{Cl}_2$  in the presence of *p*-benzoquinone (3 equivalents). The expected hybrid compound **9** was formed along with a mixture of by-products with the same or similar  $R_f$  values, necessitating its purification by preparative HPLC.<sup>[24,25]</sup>

Another intriguing feature was observed in earlier attempts to effect desulfurization on **9**. Squamoquinone **14** was obtained as expected but was eventually found to be in equilibrium with another compound. NMR spectroscopic studies of the mixture in  $\text{CDCl}_3$  supports the structure cyclo-**14** (Scheme 6).

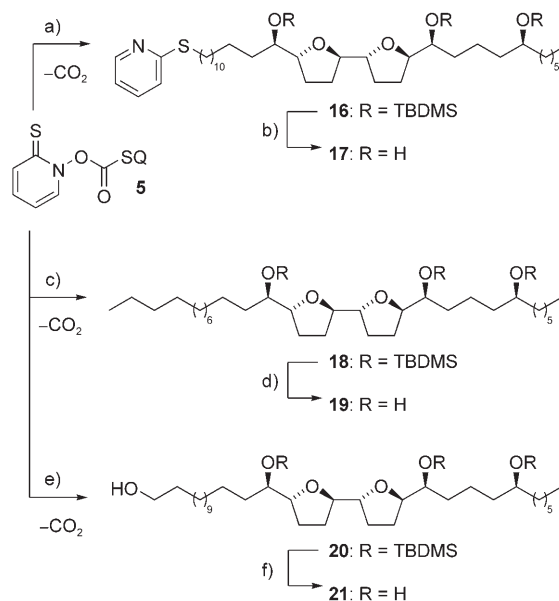


**Scheme 6.** Formation of **14** from **9**: Raney nickel (10 equiv *m/m*), THF, reflux, 15 min (50%);  $^1\text{H}$  NMR (400 MHz,  $\text{CDCl}_3$ ): splitting patterns and shifts ( $\delta$ , ppm) are indicated.

These observations can be mechanistically rationalized with the assumption that a cyclic hydroquinone derivative can be generated by intramolecular Michael addition of one secondary hydroxy function (presumably that at C19) onto the quinone nucleus. In fact, a benzylic methylene group adjacent to the hydroquinone may explain the de-shielded triplet ( $\delta = 2.53$  ppm) in comparison with the corresponding signal in the spectra of **14** ( $\delta = 2.41$  ppm). The regioselectivity of the addition may be deduced from the appearance of two singlets ( $\delta = 6.61$  and  $6.89$  ppm), which indicate two uncoupled protons. Further studies aimed at a better understanding of the formation of cyclo-**14** and its synthesis as a sole product are underway. The interest in such cyclic quinones is exemplified by the promising antitumor and pro-apoptotic properties of ansamycins.<sup>[26,27]</sup>

Full exploitation of background reactions in radical decarboxylation and quinone addition. The chemical diversity was expanded by exploiting a few side reactions of the photochemical process. Indeed, the yield of radical decarboxylation and quinone addition is constantly diminished by parasitic terminal reactions, which give further analogues that can be considered worthy of biological evaluation.

Thus, the decarboxylative rearrangement product of thiohydroxamic ester **5** (that is, protected squamocin–thiopyridine **16**) was isolated and characterized as a constant yet minor by-product, regardless of the quinone type. From a biological point of view, such a pyridine derivative could be effective as a complex I inhibitor (for example, 1-methyl-4-phenylpyridinium,  $\text{MPP}^+$ ).<sup>[24]</sup> Sulfide **16** was obtained by photochemistry<sup>[25]</sup> after exposure of ester **5** to light in  $\text{CH}_2\text{Cl}_2$  in the absence of a radical scavenger (Scheme 7). Eventually, TBDMS groups were removed by using the conditions previously described, to afford **17**.



**Scheme 7.** Synthesis of additional squamocin analogues under photochemical conditions: a)  $h\nu$ ,  $\text{CH}_2\text{Cl}_2$ ,  $0-10^\circ\text{C}$ , 1 h (24%); b) HF (75 equiv),  $\text{CH}_3\text{CN}/\text{CH}_2\text{Cl}_2$  (1:5), RT, 45 min (75%); c)  $h\nu$ , thiophenol (3 equiv),  $\text{CH}_2\text{Cl}_2$ ,  $0-10^\circ\text{C}$ , 1 h (50%); d) HF (75 equiv),  $\text{CH}_3\text{CN}/\text{CH}_2\text{Cl}_2$  (1:5), RT, 45 min (100%); e)  $h\nu$ , *tert*-butanethiol (4 equiv),  $\text{CH}_2\text{Cl}_2$ , air,  $0-10^\circ\text{C}$ , 1 h and  $\text{PPh}_3$  (1.5 equiv) (60%); f) HF (75 equiv),  $\text{CH}_3\text{CN}/\text{CH}_2\text{Cl}_2$  (1:5), RT, 45 min (83%).

The conversion of a carboxylic acid group into an alcohol with the loss of a carbon atom ( $\text{R}-\text{CO}_2\text{H} \rightarrow \text{ROH}$ ) is normally a multistep procedure. Radical decarboxylation provides a convenient alternative to existing methods, with triplet oxygen as an excellent radicophile. In the presence of a thiol group, the hydroperoxy radical generated can be reduced in situ into the corresponding hydroperoxide, which in turn can be reduced to an alcohol with excess thiol.<sup>[28]</sup> Regarding the squamocin substrate, photodecarboxylation was simply performed in  $\text{CH}_2\text{Cl}_2$  with air bubbling in the presence of excess *tert*-butyl thiol. Thus, ester **5** was converted into alcohol **20** (60% yield, Scheme 7). Final deprotection led to “squamocinol” **21**.

Recently, terminally unsubstituted acetogenins, obtained through a long total synthesis, were introduced as potent inhibitors of complex I by Miyoshi and co-workers.<sup>[9]</sup> However, the global significance of this result remains ambiguous. To address this issue, an efficient and versatile semisynthetic access to representative lactone-devoid acetogenins must be developed. To quickly and efficiently obtain such compounds, we

again used the radical decarboxylation procedure. Light exposure initiated the smooth decarboxylation of **5**, and a slight excess of thiophenol as a proton source allowed formation of the corresponding noralkane-type derivative **18** with 50% yield (Scheme 7).<sup>[18,29]</sup> As usual, the TBDMS protecting groups were removed to afford  $\Delta$ lac-squamocin **19**.

### Biological investigations

Highly cytotoxic acetogenins, including squamocin, have been described as pro-apoptotic inducers.<sup>[2]</sup> Although this phenomenon is likely to be linked to the impairment of complex I activity, such a correlation has not been demonstrated so far. Therefore, we evaluated the pro-apoptotic potential of squamocin and its analogues; representative compounds were selected, and their inhibition of mitochondrial complex I was measured. The promising compound squamoquinone **14** was selected for further studies of apoptotic processes.

**Evaluation of the pro-apoptotic potential of squamocin and its derivatives.** Cells undergoing apoptosis show an early disruption of mitochondrial transmembrane potential (MTP,  $\Delta\Psi_m$ ).<sup>[14]</sup> MTP dissipation can be detected with the help of cationic lipophilic dyes such as DiOC<sub>6</sub>(3). As the disruption in  $\Delta\Psi_m$  constitutes a constant event of apoptosis,<sup>[14,15,30,31]</sup> the measurement of this alteration can be used in the identification of new pro-apoptotic drugs. In this context, we used flow cytometry to screen squamocin and semisynthetic analogues for their ability to provoke MTP disruption and, consequently, to induce cell death. Double staining with propidium iodide (PI) allowed us to check cell impermeability and thereby to ensure the process observed was not necrosis. Our screening indicated that only compounds **14** and **15** possessed a higher pro-apoptotic potential than squamocin (Figure 2). The other quinone analogues that contain a thiopyridyl group (compound **9**) or a naphthoquinone (compound **11**) were far less effective than

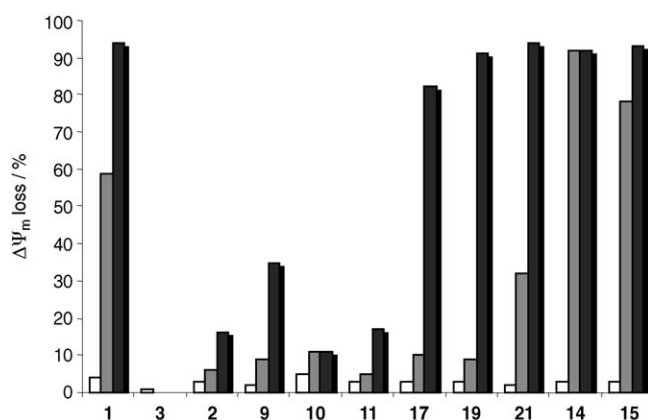


**Figure 2.** Squamocin (**1**) and its semisynthetic analogues (compound numbers indicated) provoke  $\Delta\Psi_m$  disruption in Jurkat T cells. After treatment for 24 h (white bars, 1.5  $\mu$ M; gray bars, 15  $\mu$ M; black bars, 30  $\mu$ M), Jurkat cells were labeled with both DiOC<sub>6</sub>(3) and propidium iodide (PI) and analyzed by flow cytometry. MTP loss was observed with DiOC<sub>6</sub>(3) staining. As a positive control, etoposide (10  $\mu$ M) induced  $\Delta\Psi_m$  loss on  $80 \pm 10\%$  of the cells (three independent experiments). Note that only **14** and **15** appeared to be more potent pro-apoptotic inducers than squamocin.

the natural product. The bulkiness of such functional groups could explain their decreased potency if the action of acetogenins is indeed mediated through protein inhibition. Yet as the oxidative potential of benzoquinones increases with methyl group<sup>[32]</sup> or thiophenol group substitution,<sup>[33]</sup> the redox potential of **14** exceeds that of **9** and, by extension, those of **10** and **11**. This electrochemical characteristic could influence the activity of quinone–squamocin analogues.

**Mitochondrial complex I inhibition and the pro-apoptotic potential.** Representative analogues were chosen for further investigation particularly to elucidate the potential link between the induction of apoptosis and the impairment of mitochondrial function. Their inhibitory activity toward complex I (beef heart submitochondrial particles, SMP) was evaluated by using the method previously described by Okun et al.<sup>[34]</sup> Squamocin (**1**) remained the most powerful inhibitor in comparison with analogues **9** and **14**, which were significantly less active (Table 1). Moreover, protected squamocin **3** was nearly inactive (NADH oxidase on SMP: >3000 nM) and carboxylic acid **2** resulted as a good but less potent inhibitor.

**Table 1.** Inhibition of complex I induced by squamocin and its analogues.<sup>[a]</sup>

Compound	IC <sub>50</sub> [nM]	Compound	IC <sub>50</sub> [nM]
<b>1</b>	1.3	<b>9</b>	10
<b>2</b>	40	<b>14</b>	15
<b>3</b>	> 3000	rotenone <sup>[b]</sup>	30

[a] Evaluated on bovine heart submitochondrial particles (SMP) through NADH:*n*-decylubiquinone oxidoreductase activity according to previously described methods.<sup>[34]</sup> [b] Reference inhibitor.

The lack of both pro-apoptotic potential and inhibitory activity toward complex I observed for squamocin **3** confirms that the integrity of the polyoxygenated core motif of the acetogenins is a key factor for the induction of both phenomena.<sup>[35,36]</sup> Our results show no clear relationship between complex I inhibition and the pro-apoptotic potential of acetogenin derivatives. Squamocin–carboxylic acid **2**, although a potent inhibitor of NADH:ubiquinone oxidoreductase, does not show any pro-apoptotic effect. With a likely  $pK_a$  value of  $\approx 3$ –4 under physiological pH conditions, the molecule should be negatively charged; this could prevent **2** from crossing the cellular plasma membrane to access the mitochondrion. Reciprocally, although squamoquinone **14** appears to be tenfold less potent as an inhibitor of complex I than squamocin (**1**), it is about tenfold more powerful as an apoptotic inducer on Jurkat cells, indicating an important and specific contribution of the benzoquinone moiety at the level of cellular targets other than mitochondrial complex I. The possibility of **14** being reduced to its hydroquinone form by complex I and subsequent inhibition of complex III by the resulting metabolite cannot be excluded. In that way the inhibition of both complex I and III could explain the induction of apoptosis. Furthermore, Ricci et al. recently demonstrated a link between complex I and the disruption of mitochondrial function during apoptosis.<sup>[37]</sup> Therein, the au-



thors presented the 75 kDa subunit (p75) of respiratory complex I, NDUFS1/NUAM, as a critical caspase substrate of the mitochondrial intermembrane space. Indeed, the caspase-dependent cleavage of p75 is responsible for the disruption of electron transport and  $\Delta\Psi_m$ , leading to production of radical oxygen species (ROS), loss of ATP production, and mitochondrial damage.

**Apoptotic activity of natural squamocin (1) and semisynthetic squamoquinone 14 on Jurkat T cells.** Our screening work revealed the spectacular pro-apoptotic potential of squamoquinone 14 relative to that of 1. Contrary to all expectations, despite its benzoquinone structural relationship with ubiquinone, this compound exhibited a weak inhibitory effect toward mitochondrial complex I relative to squamocin. These initial biological results encouraged us to select 14 for further studies of the apoptotic processes.

Since the report of Kerr in 1965, two types of morphologically distinct cell death have been distinguished: necrosis and apoptosis.<sup>[38]</sup> Necrosis is thought to be a passive death and inflammatory process characterized by swelling and rupture of cell membranes, dissolution of organized structures, and proteolysis. Apoptosis is a controlled biological process for the elimination of defected cells. As amphiphilic molecules, acetogenins could have been implied in a necrotic process. However the work of Zhu et al. described several characteristic features of apoptosis in the HL-60 leukemia cell line.<sup>[2]</sup> Our present work confirms and completes their results.

**Differential cytotoxic effects of natural squamocin and squamoquinone in Jurkat cells.** Previous studies have described acetogenins and particularly squamocin as impressive cytotoxic compounds on various cell lines.<sup>[39]</sup> To compare the lethal effects of squamocin and squamoquinone, Jurkat cell death was measured by flow-cytometric analysis of PI incorporation into permeabilized cells. As depicted in Figure 3, treatment with both compounds at concentrations ranging between 1 and 15  $\mu\text{M}$  for 3 to 24 h induced cell death in a dose- and time-dependant manner. Importantly, squamoquinone-induced cell death occurred more rapidly and at much lower concentrations than that brought on by squamocin. These results were confirmed by fluorescence microscopy analysis of the incorporation of Celltracker green and Hoechst 33342 into Jurkat cells treated for 6 h with squamocin at 30  $\mu\text{M}$  or squamoquinone at only 5  $\mu\text{M}$ . Indeed, the two molecules induced both a decrease in green fluorescence (which indicates the inactivation of the esterase activity responsible for sensor cleavage and fluorescence) and an increase in nuclear blue labeling that results from the condensation of chromatin in dying cells. However, whereas these features are observed in 100% of the cells treated with squamoquinone at 5  $\mu\text{M}$ , a consequent proportion of cells remained viable and could proliferate even if cultured with squamocin at 30  $\mu\text{M}$  (Figure 3B).

**Apoptotic hallmarks of cell death induced by squamocin and squamoquinone.** There are several reports in which cell death induced by acetogenins has been described as an apoptotic process.<sup>[3,4,40]</sup> Using DiOC<sub>6</sub>(3), we measured the mitochondrial membrane permeability in Jurkat cells<sup>[41,42]</sup> treated with the squamocin and squamoquinone. In parallel, aberrant surface

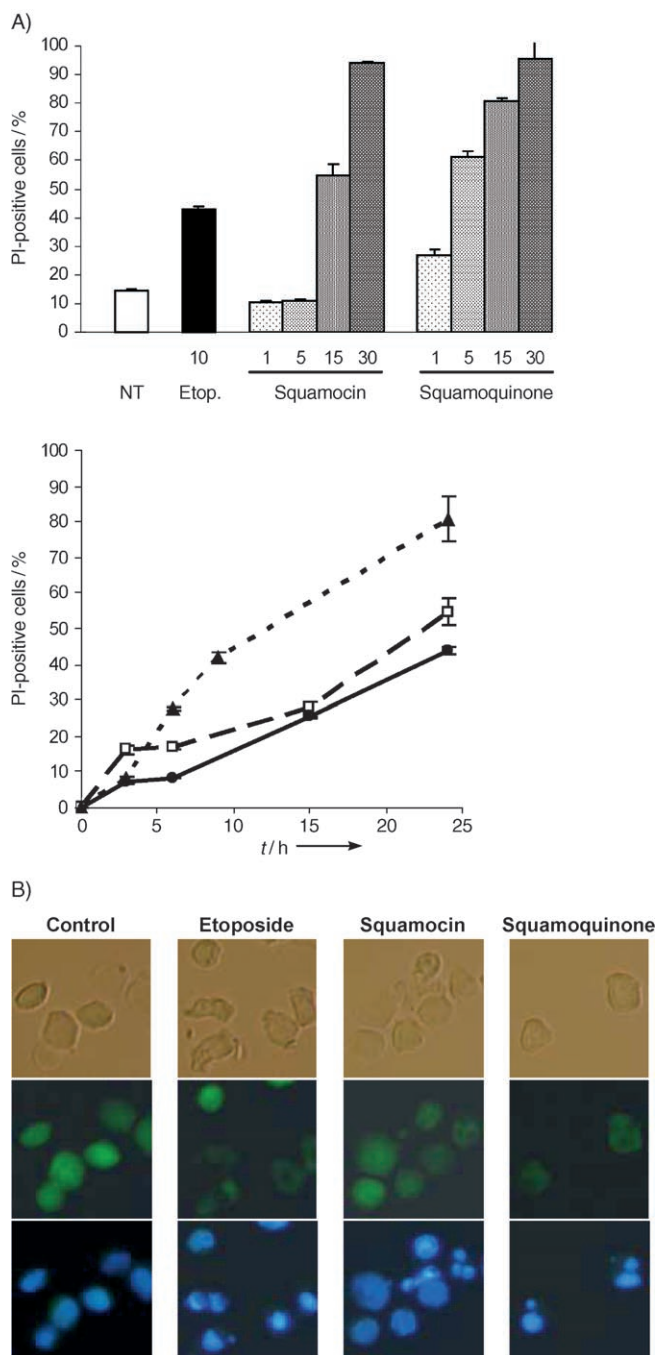


**Figure 3.** Induction of Jurkat lymphoid T cell death by squamocin and its analogue squamoquinone. A) Evaluation of nuclear permeability by a cytometric analysis of PI incorporation into chromosomal DNA. Jurkat T cells were cultured for 3–24 h in the presence of 1, 14 (1–30  $\mu\text{M}$  as indicated), or etoposide (Etop., 10  $\mu\text{M}$ ) as a positive control, followed by determination of nuclear permeability to PI to establish dose-response and time-response curves. NT: no treatment. Lower chart: etoposide, 10  $\mu\text{M}$  (—●—); squamocin, 15  $\mu\text{M}$  (---□---); squamoquinone, 15  $\mu\text{M}$  (.....▲.....). Values are means ( $\pm$  SD) of three independent experiments. B) Evaluation of cell viability by fluorescence microscopy. After treatment with squamocin (30  $\mu\text{M}$ ), squamoquinone (5  $\mu\text{M}$ ), or etoposide (40  $\mu\text{M}$ ) as a positive control, cells were stained by Celltracker green (middle row) together with Hoechst 33342 (bottom row) and examined by Hoffman modulation contrast (HMC, top row) and fluorescence microscopy. Each image shows an area of 40  $\times$  40  $\mu\text{m}^2$ .

exposure of phosphatidylserine (PS) was monitored by a fluorescent annexin V–APC conjugate (APC = allophycocyanin).<sup>[42–44]</sup> In both cases, cells were stained with PI to discriminate between healthy, apoptotic, and necrotic cells. Cellular oxidation was evaluated by labeling cells with hydroethidine (HE), which is oxidized into ethidium (Eth) following intracellular production of ROS.<sup>[41]</sup> As depicted in Figure 4, Jurkat T cells treated for 6 h with drugs at a concentration range of 1–15  $\mu\text{M}$  underwent

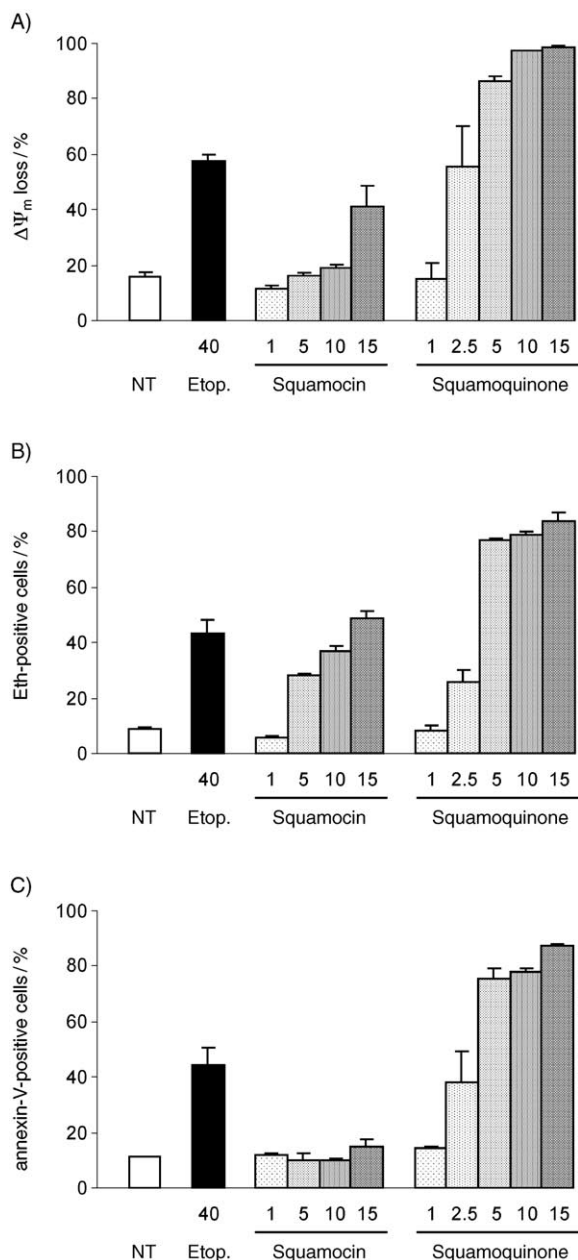


**Figure 4.** Relationship between  $\Delta\Psi_m$  disruption, ROS production and PS exposure. Determination of A)  $\Delta\Psi_m$  loss, B) ROS production, and C) PS aberrant exposure in Jurkat cells treated with squamocin, squamoquinone (1–15  $\mu\text{M}$  as indicated), or etoposide (Etop., 10  $\mu\text{M}$ ) for 6 h. NT: no treatment. After treatment, cells were labeled with DiOC<sub>6</sub>(3), HE, or annexin V. Values are means ( $\pm$  SD) obtained from three independent experiments. Squamocin and its benzoquinone analogue provoke three early events that are characteristic of apoptosis.

several features of apoptotic cell death, including  $\Delta\Psi_m$  disruption, ROS production, and finally PS exposure in a dose-dependent manner. According to the above results, the treatment with squamoquinone induced programmed cell death at lower concentrations than treatment with squamocin. Co-staining with PI confirmed that the rapid cytotoxic effects observed with squamoquinone **14** was apoptosis. Indeed, MTP decreased and PS was exposed in cells treated with **14** (2.5  $\mu\text{M}$ ) that retained their plasma membrane integrity.

*Squamocin and squamoquinone induce apoptosis through a mitochondrial pathway.* Two major signal-transduction pathways classically characterize apoptosis: the intrinsic pathway places the mitochondrion at the heart of the programmed cell death phenomenon.<sup>[45]</sup> The extrinsic pathway, commonly named the “death receptors” pathway, starts by an extracellular signal, which activates transmembrane proteins.<sup>[46]</sup> As mentioned above, squamocin is a powerful inhibitor of NADH:ubiquinone oxidoreductase. Earlier on, it seemed immediately evident that acetogenins enter cells and mitochondria, where they inhibit complex I to result in ATP deprivation and apoptosis.<sup>[39]</sup> However, ATP depletion could equally block apoptosis; complex I inhibition could also be responsible for necrosis, and another target, not necessary mitochondrial, could be implied in apoptosis.<sup>[47–49]</sup> Recently, for the first time, the synthesis of fluorescent acetogenins has allowed our research group to confirm that squamocin enters cells, with mitochondria as the primary target.<sup>[12]</sup> Mitochondria play a central role in the control of cell life and death and can kill by 1) the disruption of electron transport, oxidative phosphorylation, and adenosine triphosphate (ATP) production; 2) the release of proteins that trigger the activation of the caspase family proteases; and 3) the alteration of cellular redox potential.<sup>[45]</sup>

To explore the involvement of mitochondria in the lethal processing of **1** and **14**, we evaluated the conformational activation of the pro-apoptotic Bak protein by immunofluorescence in Jurkat cells treated with both compounds for 6 h, by means of an N-terminus-targeted anti-Bak monoclonal antibody. As observed in etoposide-treated cells, and as is depicted in Figure 5A, mitochondrial Bak is detected in its activated form in cells treated with squamocin or squamoquinone. Nuclear apoptotic bodies, characteristic of late-stage events in the apoptotic process, are concomitantly formed (Figure 5A). To assess the regulatory function of the Bcl-2 family of proteins,<sup>[50]</sup> we then used Jurkat cells in which either the anti-apoptotic Bcl-2 (Jurkat/Bcl-2) or Bcl-xL (Jurkat/Bcl-xL) proteins are overexpressed. In comparison with cells transfected with the vector alone (Jurkat/neo), only Jurkat/Bcl-xL cells showed a marked protective effect on  $\Delta\Psi_m$  disruption induced by squamocin (15  $\mu\text{M}$ ) or squamoquinone (2.5  $\mu\text{M}$ , Figure 5B). In contrast, Bcl-2 overexpression did not confer any protection against the cytotoxic effects of either compound, whereas it partially protected Jurkat cells from etoposide-mediated cellular stress. The two anti-apoptotic molecules are known to exert different protective activity, which depends on the mode of apoptosis induction. Accumulating data present Bcl-2 as a crucial protector against stress-induced apoptosis, probably resulting from its indiscriminant localization at the endoplasmic re-

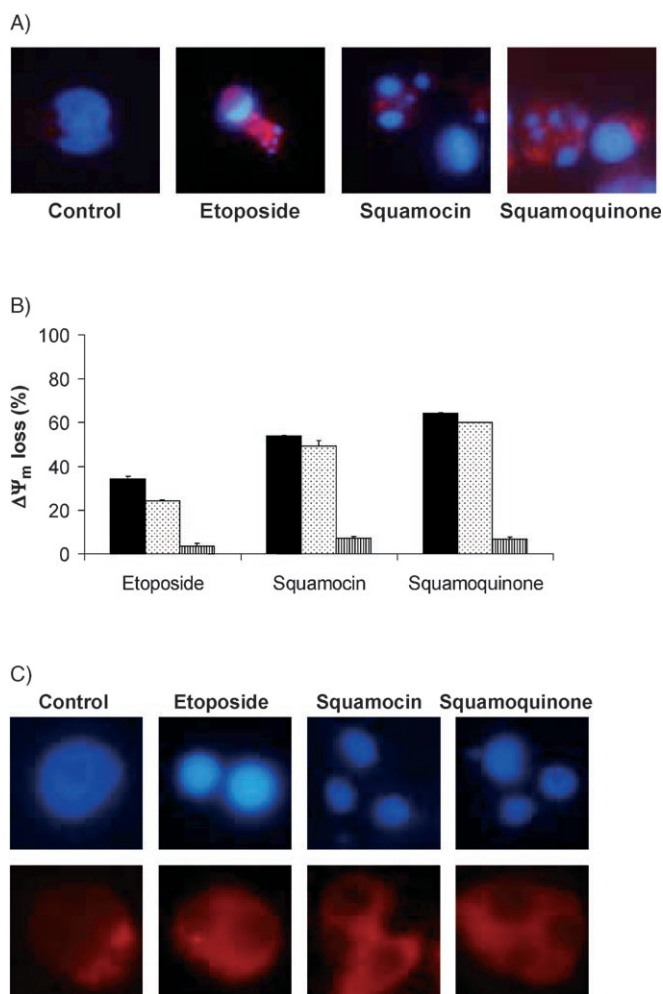


**Figure 5.** Role of mitochondria and Bcl-2 family proteins in apoptosis induced by squamocin and its analogue **14**. A) The activated form of the pro-apoptotic protein Bak was detected by immunofluorescence (red-labeled regions) concomitantly with nuclear condensation (Hoechst 33342, blue-labeled regions) after treatment of Jurkat T cells with squamocin (15  $\mu\text{M}$ ) or squamoquinone (5  $\mu\text{M}$ ) for 6 h; etoposide (10  $\mu\text{M}$ ) was chosen as a positive control. Each image shows an area of  $20 \times 20 \mu\text{m}^2$ . B) The overexpression of Bcl-xL (hashed bars) in Jurkat T cells prevents  $\Delta\Psi_m$  loss (determined by percentage of cells low in DiOC<sub>6</sub>(3)) whereas Bcl-2 (dotted bars), another member of the anti-apoptotic Bcl-2 family of proteins, does not; data collected following apoptosis after treatment with squamocin (15  $\mu\text{M}$ ), squamoquinone (2.5  $\mu\text{M}$ ), or etoposide (40  $\mu\text{M}$ ) as a positive control for 6 h. Black bars: negative control cells transfected with vector alone. Values are means ( $\pm$  SD) obtained from three independent experiments. C) The role of mitochondria in apoptosis induced by squamocin or squamoquinone is confirmed by immunofluorescence analysis, as the perinuclear staining for cytochrome c in control Jurkat T cells changed to a diffuse pattern of cytosolic staining in cells treated with squamocin (15  $\mu\text{M}$ ) or its analogue **14** (5  $\mu\text{M}$ ) for 6 h. Etoposide (10  $\mu\text{M}$ ) was chosen as a positive control. Top row: Hoechst 33342; bottom row: anti-cytochrome c immunofluorescence. Each image shows an area of  $10 \times 10 \mu\text{m}^2$ .

ticulum (ER), mitochondrial, and nuclear membranes.<sup>[51]</sup> At the mitochondrial level, Bcl-2 generally inhibits the loss of  $\Delta\Psi_m$  to a lesser extent than does Bcl-xL.<sup>[52]</sup>

The pivotal role of mitochondria in apoptosis induced by **1** and **14** is reinforced by the subcellular immunofluorescence labeling of cytochrome c. Upon release into the cytosol, cyto-

chrome c associates with Apaf-1 and with the inactive pro-caspase 9 in an ATP-dependent manner to form a complex called an "apoptosome", which induces the cleavage and the subsequent activation of caspase 9. This enzyme, as a leading activator of the caspase family of cysteine proteases, initiates the caspase cascade, which terminates in the activation of the effector caspases, including caspases 3, 6, and 7. These latter are responsible for the cleavage of various cellular substrates and carry out oligonucleosomal DNA fragmentation, leading to the apoptotic cell morphology. Indeed, in Jurkat cells treated with squamocin or squamoquinone for 6 h, and as is the case for etoposide-treated cells, the diffused (cytosolic) pattern of cytochrome c contrasts with the mitochondrial-intensive labeling observed in control cells (Figure 5C). Altogether, these data demonstrate the implication of the Bcl-2 family of proteins, particularly the Bak-Bcl-xL heterodimer, in mitochondrial matrix swelling, outer mitochondrial membrane disruption, and the cytosolic apoptotic processing provoked by squamocin and its derivative **14**.

*Squamocin and squamoquinone induce caspase-dependent DNA fragmentation.* The above results argue in favor of the activation of a direct mitochondrial pathway following treatment with compounds **1** and **14**. We next assessed the integrity of DNA in treated Jurkat cells by agarose gel electrophoresis. As shown in Figure 6A and B, both oligonucleosomal and large-scale ( $\approx 50$  kb) DNA fragmentations were observed in Jurkat cells treated with etoposide, as well as squamocin and squamoquinone. This was correlated with the appearance of cells with a hypo-diploid DNA content (sub-G<sub>1</sub>) after treatment in the same conditions for 24 h (Figure 6C). Importantly, both fragmentations were abolished if cells were pre-treated with the general caspase inhibitor z-VAD.fmk, suggesting that the mitochondrial alterations essentially lead to caspase-dependent nuclear apoptosis (Figure 6A and B). Moreover, and as pointed out in Figure 6D, mitochondrial permeability and PS exposure induced by squamocin and **14** were decreased by pre-treatment with z-VAD.fmk. Similarly, z-DEVD.fmk (an inhibitor of caspase 3 and caspase 7) and z-LEHD.fmk (a caspase 9 inhibitor) were also able to block the programmed cell-death process activated by **1** and **14**. This implies that, as with cells dying from classical apoptosis, the effector caspase 3 and initiator caspase 9 are activated in squamocin- and squamoquinone-treated cells following mitochondrial depolarization, affecting both cytosolic and nuclear integrity.

## Conclusions

The chemistry described herein resulted in a flexible and rapid preparation of a small focused library of analogues of natural squamocin (**1**). As a cornerstone of our strategy, the radical decarboxylation and quinone addition reaction found its utility as an interesting reaction in the design of natural-product-like compounds. It was effective and reliable in the transformation of a long fatty-acid-like substrate (C<sub>32</sub>) for which conventional methods have often failed. Hybrid **14**, squamoquinone, emerged from the pro-apoptotic screening as a promising compound. We demonstrate that, like squamocin, **14** induces



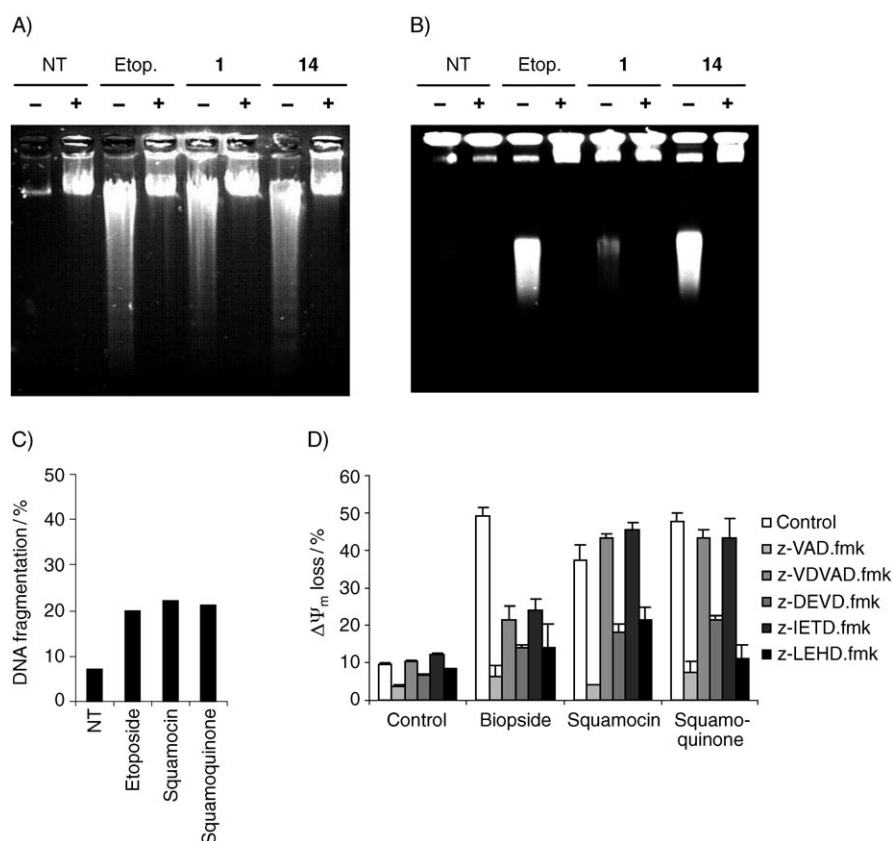


**Figure 6.** Caspase-dependent nuclear apoptosis induced by etoposide, squamocin, or squamoquinone in Jurkat cells. A) Determination of oligonucleosomal DNA fragmentation in Jurkat cells after treatment with squamocin (**1**, 15  $\mu\text{M}$ ), squamoquinone (**14**, 2.5  $\mu\text{M}$ ), or etoposide (Etop., 40  $\mu\text{M}$ ) in the presence (+) or absence (–) of z-VAD.fmk (50  $\mu\text{M}$ ) for 16 h; NT: no treatment. B) Assessment of large-scale DNA fragmentation by field inversion gel electrophoresis (FIGE) in Jurkat cells treated as described in part A). Note that squamocin and squamoquinone along with etoposide induce DNA fragmentation that is blocked by the z-VAD.fmk caspase inhibitor. C) After treatment of Jurkat cells with squamocin (15  $\mu\text{M}$ ), squamoquinone (2.5  $\mu\text{M}$ ), or etoposide (40  $\mu\text{M}$ ), cells were harvested, alcohol-fixed and stained with PI. DNA fragmentation is expressed as the percentage of cells with hypo-diploid DNA. Similar to the effects etoposide, **1** and **14** induce  $\approx 20\%$  of the cells with sub-diploid DNA content (sub- $G_1$ ). D) The effect of several caspase inhibitors was evaluated by the incubation of Jurkat cells initially with z-VAD.fmk, z-VDVAD.fmk, z-DEVD.fmk, z-IETD.fmk, or z-LEHD.fmk (50  $\mu\text{M}$  each), inhibitors of caspases in general, caspases 2, 3, 8, and 9, respectively. Then after treatment with squamocin (30  $\mu\text{M}$ ), squamoquinone (2.5  $\mu\text{M}$ ), or etoposide (40  $\mu\text{M}$ ) for 6 h, the percentage of cells with  $\Delta\Psi_m$  loss and PS aberrant exposure was determined by flow cytometry after staining with both DiOC<sub>6</sub>(3) and annexin V-APC. Values were determined from annexin V-APC-positive cells and are means ( $\pm$  SD) obtained from three independent experiments. Inhibitors of caspases 3 and 9 are able to block apoptosis caused by squamocin or squamoquinone.

apoptosis in a classical mitochondrial caspase-dependent pathway in Jurkat lymphoid T cells. Squamoquinone is tenfold more potent than its naturally occurring precursor. However, with regard to the discrepancy between complex I inhibition and apoptotic processing, a direct effect of squamocin and squamoquinone on mitochondrial membrane structure cannot be ruled out.<sup>[5]</sup> Such an effect by **1** and **14** may be due to their own properties of interaction with lipid membranes,<sup>[12,53]</sup> and may lead to the disruption of the Bak–Bcl-xL heterodimer in the mitochondrial outer membrane, leading to the conformational activation of Bak, membrane depolarization, and apoptotic processing.<sup>[54]</sup> Further experiments based on Bcl-xL levels and localization are needed to explore this hypothesis, but this may explain the stronger protective effect of Bcl-xL in comparison with Bcl-2 in cells treated with our squamocin compounds.

## Experimental Section

**Chemistry.** General procedures: All reactions were carried out under an argon atmosphere with dry solvents under anhydrous conditions. Yields refer to chromatographically and spectroscopically homogeneous materials, unless otherwise stated. Reactions were monitored by thin-layer chromatography (TLC) carried out on Kieselgel silica gel plates (60F-254, Merck) with UV light as the visualizing agent if required, and sulfuric vanillin reagent and heat as developing agent. Kieselgel silica gel (60, particle size 40–63  $\mu\text{m}$ , Merck) was used for flash chromatography.

Tri-OTBDMS squamocin **3**: 4-Dimethylaminopyridine (DMAP, cat.) and squamocin (1.015 g, 1.63 mmol) were mixed in pyridine (15 mL). At 0 °C, *tert*-butyldimethylsilyl trifluoromethanesulfonate (1.725 g, 1.5 mL, 6.53 mmol, 4 equiv) was added dropwise, and the mixture was stirred at room temperature for 2 h. After dilution with water, the mixture was extracted with diethyl ether (5  $\times$  20 mL). The combined organic layers were dried (Na<sub>2</sub>SO<sub>4</sub>), filtered, and concentrated under decreased pressure. The crude mixture was then purified by flash chromatography on silica gel (C<sub>6</sub>H<sub>12</sub>/AcOEt 95:5) to give **3** (1.058 g, 80%).

Preparation of carboxylic acids **2** and **4**: squamocin (**1**) (589 mg, 0.95 mmol) or protected squamocin **3** (1.611 g, 1.67 mmol) was dissolved in acetone. KMnO<sub>4</sub> (4 equiv) was dissolved in water and added to the mixture under vigorous stirring. After 24 h at room temperature, MnO<sub>2</sub> was filtered and acetone evaporated. The aqueous layer, adjusted to pH 4 with a solution of citric acid (4%), was extracted with CH<sub>2</sub>Cl<sub>2</sub>. The combined organic layers were dried (Na<sub>2</sub>SO<sub>4</sub>) and concentrated under decreased pressure. The crude mixture was then purified by flash chromatography on silica gel (CH<sub>2</sub>Cl<sub>2</sub>/MeOH 95:5) for **2** (330 mg, 60%) and (C<sub>6</sub>H<sub>12</sub>/AcOEt 9:1) for **4** (1.010 g, 70%).

Preparation of the unprotected thiohydroxamic ester derivative and protected thiohydroxamic ester **5**: In a flask protected from light, carboxylic acid **4** or **2** and 2-thiopyridine-*N*-oxide (20 equiv for **2** and 1.2 equiv for **4**) were mixed in CH<sub>2</sub>Cl<sub>2</sub> (10 mL) at 0 °C. DCC (2 equiv) was added slowly, and the mixture was stirred at room temperature overnight. After completion of the reaction, *N,N*-dicyclohexylurea (DCU) was removed by filtration on a celite column. The filtrate was concentrated under decreased pressure at 30 °C. The crude mixture was purified by flash chromatography

(CH<sub>2</sub>Cl<sub>2</sub>/MeOH 98:2 for unprotected thiohydroxamic ester, C<sub>6</sub>H<sub>12</sub>/Et<sub>2</sub>O 7:3 for **5**) leading to **2** (128 mg, 75%) or **5** (220 mg, 80%).

Radical decarboxylation and quinone addition to give **6–8**: In a pyrex tube, **5** and the appropriate quinone (3 equiv) were mixed in CH<sub>2</sub>Cl<sub>2</sub> (2 mL). The reaction mixture was subsequently exposed to light from a halogen lamp (500 W) placed ≈20 cm away while maintaining the temperature between 0 and 10 °C. After completion of the reaction (≈1 h, monitored by TLC), the reaction mixture was diluted with CH<sub>2</sub>Cl<sub>2</sub> (20 mL), and the remaining quinone extracted in its hydroquinone form by a saturated solution of sodium thiosulfate (4×40 mL). The organic layer was dried (Na<sub>2</sub>SO<sub>4</sub>), filtered through a small MnO<sub>2</sub> column, and concentrated under decreased pressure. The crude mixture was then purified by flash chromatography (C<sub>6</sub>H<sub>12</sub>/AcOEt 97:3) to give **6** (120 mg, 51%), **7** (59 mg, 54%) or **8** (55 mg, 39%).

Elimination of the thiopyridyl group to obtain **12** and **13**: A solution of quinone **6** (21 mg, 0.019 mmol) or **7** (16 mg, 0.015 mmol) in dry THF (2 mL) was treated with excess Raney nickel (W-2, 50% slurry in water, 200 mg) at reflux for 45 min. The reaction mixture was then filtered through a small celite column, washed with CH<sub>2</sub>Cl<sub>2</sub> and Et<sub>2</sub>O, and the filtrate was concentrated under decreased pressure. The residue was dissolved in CH<sub>2</sub>Cl<sub>2</sub> (4 mL) and washed with a solution of aqueous copper sulfate (10%, 3×5 mL) and then water (2×5 mL). The organic fraction was dried (Na<sub>2</sub>SO<sub>4</sub>) and concentrated under decreased pressure. The residue was treated with excess MnO<sub>2</sub> (50 mg) while stirring in CH<sub>2</sub>Cl<sub>2</sub> at room temperature for 15 min for oxidation, filtered on a small celite column, and concentrated to give **12** (13 mg, 69%) or **13** (12 mg, 80%).

Radical rearrangement of **5** into **16**: In a pyrex tube, thiohydroxamic ester **5** (44 mg, 0.043 mmol) was dissolved in benzene (2 mL, (caution!)). The reaction mixture was exposed to light from a halogen lamp (500 W) placed ≈20 cm away while maintaining the temperature between 0 and 10 °C. At the end of the reaction (≈10 min, monitored by TLC), the mixture was concentrated under decreased pressure, dissolved in CH<sub>2</sub>Cl<sub>2</sub>, and washed with a solution of aqueous copper sulfate (10%). The organic layer was dried (Na<sub>2</sub>SO<sub>4</sub>) and concentrated under decreased pressure. The residue was then purified by flash chromatography (C<sub>6</sub>H<sub>12</sub>/AcOEt 99:1, 95:5, and 8:2) to give **16** (10 mg, 24%).

Radical decarboxylative hydroxylation to afford **20**: *tert*-butanethiol (18 mg, 22 μL, 0.204 mmol, 4 equiv) was added to a solution of **5** (52 mg, 0.051 mmol) in toluene (5 mL) at 0 °C. The reaction mixture, stirred under air bubbling, was exposed to light from a halogen lamp (500 W) placed ≈20 cm away for 1 h. Triphenylphosphine (20 mg, 0.077 mmol, 1.5 equiv) was added, and the mixture was stirred for 5 min. The solvent was evaporated under decreased pressure, and the residue was purified by flash chromatography (C<sub>6</sub>H<sub>12</sub>/AcOEt 97:3) to give **20** (27 mg, 60%).

Radical reduction to afford **18**: Thiophenol (5 mg, 5 μL, 0.048 mmol, 3 equiv) was added to a solution of thiohydroxamic ester **5** (16 mg, 0.016 mmol) in CH<sub>2</sub>Cl<sub>2</sub> at 0 °C. The reaction mixture was exposed to light from a halogen lamp (500 W) placed ≈20 cm away for 1 h with the temperature kept between 0 and 10 °C. At the end of the reaction, the organic layer was washed with an aqueous saturated solution of NaHCO<sub>3</sub>, dried (Na<sub>2</sub>SO<sub>4</sub>), and concentrated under decreased pressure. The residue was purified by flash chromatography (C<sub>6</sub>H<sub>12</sub> followed by C<sub>6</sub>H<sub>12</sub>/AcOEt 95:5) to give **18** (7 mg, 50%).

Elimination of TBDMS groups to afford **2, 9–11, 14, 15, 17, 19** and **21**: to a solution of silylated compound (**4**: 20 mg, 22 μmol; **6**:

**73** mg, 67 μmol; **7**: 15 mg, 14 μmol; **8**: 47 mg, 42 μmol; **12**: 11 mg, 11 μmol; **13**: 10 mg, 10 μmol; **16**: 6 mg, 6 μmol; **18**: 6 mg, 7 μmol; **20**: 10 mg, 11 μmol) in CH<sub>2</sub>Cl<sub>2</sub>/CH<sub>3</sub>CN (5:1) in an ice bath, HF was added dropwise (50% aq., 75 equiv). The mixture was stirred at room temperature for 45 min and quenched with an aqueous saturated solution of NaHCO<sub>3</sub>. The deprotected product was extracted with CH<sub>2</sub>Cl<sub>2</sub> (3×5 mL), and the combined organic layers were washed with an aqueous saturated solution of NaHCO<sub>3</sub> (3×10 mL) and concentrated under decreased pressure to give **2** (11 mg, 90%), **9** (42 mg, 86%), **10** (4.5 mg, 43%), **11** (32 mg, 97%), **14** (5 mg, 70%), **15** (5 mg, 77%), **17** (3 mg, 75%), **19** (4 mg, 100%), and **21** (5 mg, 83%).

**Biology.** Cell culture and treatments: Jurkat cells (clone E6–1) were cultured in complete culture medium (RPMI 1640 supplemented with 10% fetal calf serum (FCS), L-glutamine (2 mM), and penicillin/streptomycin (100 U mL<sup>-1</sup> each)) and maintained at 37 °C in a humidified atmosphere of CO<sub>2</sub> (5%). For the screening of squamocin derivatives, cells were cultured to a density of 5×10<sup>5</sup> mL<sup>-1</sup> on flat-bottomed 96-well plates (Nunc). 10<sup>5</sup> cells (200 μL) per well were treated with a given derivative (1.5, 15 and 30 μM) for 24 h. For the characterization of apoptotic pathways, Jurkat cells at a density of 5×10<sup>5</sup> mL<sup>-1</sup> were treated with compounds **1** or **14** in a concentration range of 1–30 μM for 1–24 h. To avoid practical problems linked with the particular physicochemistry of acetogenins, each derivative was distributed in absolute ethanol (10 mM) and diluted in complete culture medium to a final concentration of 60 μM. Of this, 100 μL were added to 100 μL of cultured cell suspension (10<sup>6</sup> cells mL<sup>-1</sup>) to afford the dilution at 30 μM. Apoptosis was induced by treatment of cells with the topoisomerase II inhibitor etoposide (Sigma–Aldrich, St. Louis, USA); apoptosis was inhibited by pre-incubation (30 min) with the general caspase inhibitor z-VAD.fmk (50 μM), the caspase 3 and caspase 7 inhibitor z-DEVD.fmk, the caspase 2 inhibitor z-VDVAD.fmk, the caspase 9 inhibitor z-LEHD.fmk, or the caspase 8 and caspase 10 inhibitor z-IETD.fmk (all from Enzyme Systems Products, Livermore, USA).

Cytofluorometric determination of cell death: To evaluate cell permeability, control and treated cells were stained with propidium iodide (0.5 μg mL<sup>-1</sup>, Sigma–Aldrich, St. Louis, USA), and the fluorochrome incorporation was immediately analyzed on a flow cytometer (FACSCalibur, BD Biosciences, San Jose, USA). ΔΨ<sub>m</sub> was measured after incubating cells at 37 °C for 15 min with the cationic lipophilic fluorochrome DiOC<sub>6</sub>(3) (40 nM, Sigma–Aldrich, St. Louis, USA). In parallel, cells were also stained with hydroethidine (2 μM, Molecular Probes, Eugene, USA) and with an annexin V–APC conjugate (1 μL, Bender Medsystems, Vienna, Austria) to measure the generation of superoxide anion and to assess aberrant PS exposure, respectively. For quantitation of hypo-diploid cells, Jurkat cells were treated with squamocin (15 μM), its derivative **14** (2.5 μM), or etoposide (40 μM) for 24 h. After two washes in phosphate-buffered saline (PBS), cells were fixed with ethanol (70%) and placed overnight at –20 °C. Prior to analysis, cells were washed, re-suspended in PBS containing RNase A (100 μg mL<sup>-1</sup>) and PI (2 μg mL<sup>-1</sup>),<sup>[55]</sup> and immediately analyzed by flow cytometry. For each labeling, a total of 10 000 events were considered.

Bcl-2 and Bcl-xL overexpression: Jurkat cells were stably transfected either with pcDNA3.1 control vector (*Neo*), or with pcDNA3.1-subcloned human *Bcl-2* and *Bcl-xL* inserts, kindly provided by Dr. J. L. Fernandez-Luna (University Hospital of Santander, Spain).<sup>[56]</sup>

Fluorescence microscopy: After treatment with squamocin (30 μM) or its benzoquinone analogue **14** (5 μM) for 6 h, Jurkat cell viability was evaluated with the viability sensor Celltracker (Molecular

Probes). Briefly, harvested cells were stained at 37 °C for 15 min with the fluorescent probe (10 mM), washed in PBS, and fixed with paraformaldehyde (1%) for 15 min. After a second wash in PBS, cells were centrifuged on glass cover-slips coated with poly-L-lysine, counterstained for DNA detection with Hoechst 33342 (1  $\mu$ M, Sigma–Aldrich, St. Louis, USA), and mounted in Mowiol (Calbiochem, La Jolla, USA). Preparations were observed with a Nikon Eclipse TE2000-U microscope, and analyzed with Nikon ACT-1 software. For immunofluorescent labeling of intracellular Bak and cytochrome c, Jurkat cells were treated with squamocin (15  $\mu$ M) or its benzoquinone analogue **14** (5  $\mu$ M) for 6 h, and then prepared on glass cover-slips coated with poly-L-lysine, as described above. Cover-slips were washed twice in PBS, and cells were briefly permeabilized with PBS containing saponin (0.1%), as described previously.<sup>[57]</sup> A mouse-derived antiserum against Bak or cytochrome c was added to permeabilized cells (1/100 and 1/150, respectively, BD Pharmingen, San Diego, USA), and monitored with a goat anti-mouse IgG conjugated to TRITC (1/150, Sigma–Aldrich, St. Louis, USA). Cover-slips were then mounted and analyzed as above.

**DNA gel electrophoresis:** For field inversion gel electrophoresis (FIGE), cells were treated with squamocin (15  $\mu$ M) or its benzoquinone analogue **14** (2.5  $\mu$ M) for 6 h, washed once in PBS, and included in agarose plugs ( $2 \times 10^6$  cells). DNA was then prepared as previously described,<sup>[58]</sup> and separated on a FIGE Mapper cell (1% agarose, 0.5  $\times$  TBE, Bio-Rad Laboratories). Running conditions: 180 V (forward pulse), 120 V (reverse pulse), and 1.5 and 3.5 s for the initial and final switch times (forward and reverse pulses, linear ramp) for 20 h. For the detection of nucleosomal DNA fragmentation, DNA was extracted from lysed cells according to standard protocols in the presence of protease K and RNase A, and then subjected to conventional horizontal agarose gel electrophoresis (1.8%, TAE) followed by staining with ethidium bromide.

## Acknowledgments

This work was supported by grants from the Ministère de la recherche (S.D.), the Association pour la Recherche sur le Cancer (contract 4812), Fondation de France, Fondation pour la Recherche Médicale, Ligue Nationale contre le Cancer, and the Pasteur–Weizmann Scientific Council (S.A.S.). We thank Jean-Christophe Jullian for assistance with NMR spectroscopy. We are grateful to Professor C. Labarre, Dr. C. Sandre, and Mrs. R. Gorges-Kergot from the Département de microbiologie et immunologie (Faculté de Pharmacie, Châtenay-Malabry, France) for assistance in cytometry and cell culture.

**Keywords:** acetogenin • apoptosis • caspases • quinones • radical reactions

- [1] J. K. Rupprecht, Y.-H. Hui, J. L. McLaughlin, *J. Nat. Prod.* **1990**, *53*, 237–278.
- [2] X.-F. Zhu, Z.-C. Liu, B.-F. Xie, Z.-M. Li, G.-K. Feng, H.-H. Xie, S.-J. Wu, R.-Z. Yang, X.-Y. Wei, Y.-X. Zeng, *Life Sci.* **2002**, *70*, 1259–1269.
- [3] H.-F. Chiu, T.-T. Chih, Y.-M. Hsian, C.-H. Tseng, M.-J. Wu, Y.-C. Wu, *Biochem. Pharmacol.* **2003**, *65*, 319–327.
- [4] S.-S. F. Yuan, H.-L. Chang, H.-W. Chen, Y.-T. Yeh, Y.-H. Kao, K.-H. Lin, Y.-C. Wu, J.-H. Su, *Life Sci.* **2003**, *72*, 2853–2861.
- [5] E. J. Wolvetang, K. L. Johnson, K. Krauer, S. J. Ralph, A. W. Linnane, *FEBS Lett.* **1994**, *339*, 40–44.
- [6] S. Rodier, Y. Le Huerou, B. Renoux, J. Doyon, P. Renard, A. Pierre, J. P. Gesson, R. Grée, *Anti-Cancer Drug Des.* **2001**, *16*, 109–117.
- [7] H. Miyoshi, M. Ohshima, H. Shimada, T. Akagi, H. Iwamura, J. L. McLaughlin, *Biochim. Biophys. Acta* **1998**, *1365*, 443–452.
- [8] M. Takada, K. Kuwabara, H. Nakato, A. Tanaka, H. Iwamura, H. Miyoshi, *Biochim. Biophys. Acta* **2000**, *1460*, 302–310.
- [9] T. Hamada, N. Ichimaru, M. Abe, D. Fujita, A. Kenmochi, T. Nishioka, K. Zwicker, U. Brandt, H. Miyoshi, *Biochemistry* **2004**, *43*, 3651–3658.
- [10] S. Arndt, U. Emde, S. Baurle, T. Friedrich, L. Grubert, U. Koert, *Chem. Eur. J.* **2001**, *7*, 993–1005.
- [11] H. Yabunaka, M. Abe, A. Kenmochi, T. Hamada, T. Nishioka, H. Miyoshi, *Bioorg. Med. Chem. Lett.* **2003**, *13*, 2385–2388.
- [12] S. Derbré, G. Roué, E. Poupon, S. A. Susin, R. Hocquemiller, *ChemBioChem* **2005**, *6*, 979–982.
- [13] G. Tudor, P. Gutierrez, A. Aguilera-Gutierrez, E. A. Sausville, *Biochem. Pharmacol.* **2003**, *7583*, 1–15.
- [14] N. Zamzami, P. Marchetti, M. Castedo, D. Decaudin, A. Macho, T. Hirsch, S. A. Susin, P. X. Petit, B. Mignotte, G. Kroemer, *J. Exp. Med.* **1995**, *182*, 367–377.
- [15] N. Zamzami, S. A. Susin, P. Marchetti, T. Hirsch, I. Gomez-Monterrey, M. Castedo, G. Kroemer, *J. Exp. Med.* **1996**, *183*, 1533–1544.
- [16] M. O. Hengartner, *Nature* **2000**, *407*, 770–776.
- [17] D. H. R. Barton, D. Bridon, S. Z. Zard, *Tetrahedron* **1987**, *43*, 5307–5314.
- [18] S. I. Parekh, D. H. R. Barton in *Half a Century of Free Radical Chemistry* (Eds.: L. A. Radicati, D. Brozolo), Cambridge University Press, Cambridge, **1993**, pp. 46–90.
- [19] R. Duval, G. Lewin, R. Hocquemiller, *Bioorg. Med. Chem.* **2003**, *11*, 3439–3446.
- [20] P. Duret, A.-I. Waechter, B. Figadère, R. Hocquemiller, A. Cavé, C. Piérard, M. Peres, *Tetrahedron Lett.* **1996**, *37*, 7043–7046.
- [21] S. D. Jolad, J. J. Hoffmann, J. R. Cole, C. E. Barry, R. B. Bates, G. S. Linz, W. A. König, *J. Nat. Prod.* **1985**, *48*, 644–645.
- [22] S. O. Nwaukwa, P. M. Keehn, *Tetrahedron Lett.* **1982**, *23*, 3135–3138.
- [23] N. Morrow, C. A. Ramsden, B. J. Sargent, C. D. Walleit, *Tetrahedron* **1998**, *54*, 9603–9612.
- [24] Y. Kotake, S. Ohta, *Curr. Med. Chem.* **2003**, *10*, 2507–2516.
- [25] D. H. R. Barton, D. Crich, P. Potier, *Tetrahedron Lett.* **1985**, *26*, 5943–5946.
- [26] L. Whitesell, E. G. Mimnaugh, B. D. Costa, C. E. Myers, L. M. Neckers, *Proc. Natl. Acad. Sci. USA* **1994**, *91*, 8324–8328.
- [27] M. B. Andrus, E. J. Hicken, E. L. Meredith, B. L. Simmons, J. F. Cannon, *Org. Lett.* **2003**, *5*, 3859–3862.
- [28] D. H. R. Barton, S. D. Géro, P. Holliday, B. Quiclet-Sire, S. Z. Zard, *Tetrahedron* **1998**, *54*, 6751–6756.
- [29] J. Zhu, A. J. H. Klunder, B. Zwanenburg, *Tetrahedron* **1995**, *51*, 5099–5116.
- [30] N. Zamzami, P. Marchetti, M. Castedo, C. Zanin, J. L. Vayssière, P. X. Petit, G. Kroemer, *J. Exp. Med.* **1995**, *181*, 1661–1672.
- [31] U. Ozgen, S. Savasan, S. Buck, Y. Ravindranath, *Cytometry* **2000**, *42*, 74–78.
- [32] V. W. Flaig, H. Beutelspacher, H. Riemer, E. Kalke, *Justus Liebigs Ann. Chem.* **1968**, *719*, 96–111.
- [33] E. R. Brown, K. T. Finley, R. L. Reeves, *J. Org. Chem.* **1971**, *36*, 2849–2853.
- [34] J. G. Okun, P. Lummen, U. Brandt, *J. Biol. Chem.* **1999**, *274*, 2625–2630.
- [35] S. Rodier, Y. Le Huerou, B. Renoux, J. Doyon, P. Renard, A. Pierré, J. P. Gesson, R. Grée, *Bioorg. Med. Chem. Lett.* **2000**, *10*, 1373–1375.
- [36] P. Duret, R. Hocquemiller, J. C. Gantier, B. Figadère, *Bioorg. Med. Chem.* **1999**, *7*, 1821–1826.
- [37] J. E. Ricci, C. Munoz-Pinedo, P. Fitzgerald, B. Bailly-Maitre, G. A. Perkins, N. Yadava, I. E. Scheffler, M. H. Ellisman, D. R. Green, *Cell* **2004**, *117*, 773–786.
- [38] J. F. Kerr, *J. Pathol. Bacteriol.* **1965**, *90*, 419.
- [39] Q. Alali, X.-X. Liu, J. L. McLaughlin, *J. Nat. Prod.* **1999**, *62*, 504–540.
- [40] H.-W. Chih, H.-F. Chiu, K.-S. Tang, F.-R. Chang, Y.-C. Wu, *Life Sci.* **2001**, *69*, 1321–1331.
- [41] N. Zamzami, P. Marchetti, M. Castedo, D. Decaudin, A. Macho, T. Hirsch, S. A. Susin, P. X. Petit, B. Mignotte, G. Kroemer, *J. Exp. Med.* **1995**, *182*, 367–377.
- [42] M. Castedo, T. Hirsch, S. A. Susin, N. Zamzami, P. Marchetti, A. Macho, G. Kroemer, *J. Immunol.* **1997**, *157*, 512–521.
- [43] B. Verhoven, Schlegel, P. Williamson, *J. Exp. Med.* **1995**, *182*, 1597–1601.

- [44] S. J. Martin, C. P. M. Reutelingsperger, A. J. McGahon, J. A. Rader, R. C. A. A. Van Schie, D. M. LaFace, D. R. Green, *J. Exp. Med.* **1995**, *182*, 1545–1556.
- [45] D. R. Green, J. C. Reed, *Science* **1998**, *281*, 1309–1312.
- [46] A. Ashkenazi, V. M. Dixit, *Science* **1998**, *281*, 1305–1308.
- [47] M. Leist, B. Single, A. F. Castoldi, S. Kuhnle, P. Nicotera, *J. Exp. Med.* **1997**, *185*, 1481–1486.
- [48] G. Kroemer, B. Dallaporta, M. Resche-Rigon, *Annu. Rev. Physiol.* **1998**, *60*, 619–642.
- [49] G. R. Huang, S. Jiang, Y.-L. Wu, Y. Jin, Z.-J. Yao, J.-R. Wu, *ChemBioChem* **2003**, *4*, 1216–1221.
- [50] N. Zamzami, C. Brenner, I. Marzo, S. A. Susin, G. Kroemer, *Oncogene* **1998**, *16*, 2265–2282.
- [51] M. J. Thomenius, N. S. Wang, E. Z. Reineks, Z. Wang, C. W. Distelhorst, *J. Biol. Chem.* **2003**, *278*, 6243–6250.
- [52] R. Kim, *Biochem. Biophys. Res. Commun.* **2005**, *333*, 336–343.
- [53] H. Shimada, J. B. Grutzner, J. F. Kozlowski, J. L. McLaughlin, *Biochemistry* **1998**, *37*, 854–866.
- [54] F. Gonzalez, F. Pariselli, P. Dupaigne, I. Budihardjo, M. Lutter, B. Antonsson, P. Diolez, S. Manon, J. C. Martinou, M. Goubern, X. Wang, S. Bernard, P. X. Petit, *Cell Death Differ.* **2005**, *12*, 614–626.
- [55] R. Nunez, *Curr. Issues Mol. Biol.* **2001**, *3*, 67–70.
- [56] M. Silva, D. Grillot, A. Benito, C. Richard, G. Nuñez, J. L. Fernández-Luna, *Blood* **1996**, *88*, 1576–1582.
- [57] I. Marzo, P. Perez-Galan, P. Giraldo, D. Rubio-Felix, A. Anel, J. Naval, *Biochem. J.* **2001**, *359*, 537–546.
- [58] D. G. Brown, X. M. Sun, G. M. Cohen, *J. Biol. Chem.* **1993**, *268*, 3037–3039.

---

Received: July 19, 2005

Published online on November 4, 2005